Glaucoma in Primates: Cytochrome Oxidase Reactivity in Parvo- and Magnocellular Pathways

Morris L. J. Crawford,[1] *Ronald S. Harwerth,*[2] *Earl L. Smith III,*[2] *Fran Shen,*[1] *and Louvenia Carter-Dawson*[1]

Purpose. To evaluate the differential effects of ganglion cell depletion from experimental glaucoma on the relative metabolic activities of neurons in the parvo (P)- and magno (M)-cellular visual pathways of the macaque visual system.

Methods. Monocular experimental glaucoma was induced in monkeys (*Macaca mulatta* and *M. fascicularis*) by applying a laser to the trabecular meshwork to increase intraocular pressure (IOP). After other behavioral and electrophysiological studies, the lateral geniculate nuclei (LGNs) and the primary visual cortices were analyzed for functional afference from surviving ganglion cells, indicated by cytochrome oxidase (CO) histochemistry.

Results. CO reactivity (COR) indicated a general reduction in neural metabolism with increasing severity of glaucoma. COR in the LGNs was reduced to the same degree in both the P- and M-cellular layers. In layer 4Cβ of the V1 cortex, the reactivity was always reduced more than in the layer 4Cα division.

Conclusions. Experimental glaucoma in monkeys reduces visual afference to the central nervous system, thereby reducing the metabolic drive as indicated by COR. The detrimental effect of glaucoma did not appear to be any greater for the M-cell, rather than the P-cell pathway in the LGN or in the visual cortex. Both are affected by the duration and severity of the experimental glaucoma. Overall, the alterations in metabolism of neurons in the parallel visual pathways supplied by the Pα and Pβ ganglion cells do not suggest that tests based on the functional properties of one or the other would provide optimal assessment of glaucoma. (*Invest Ophthalmol Vis Sci.* 2000;41: 1791–1802)

Glaucoma is an optic neuropathy that results from the death of ganglion cells of the retina. It affects 4 to 10 million North Americans, and is a major cause of visual disability and blindness.[1,2] There is no agreed-on cause of the disorder, although glaucoma is often associated with elevated intraocular pressure (IOP).[3–6] Because glaucoma occurs in persons with normal IOP[7] and does not always cause elevated IOP, pressure cannot be the sole causative agent. Increased IOP may be a result rather than the cause of glaucoma initiated by other metabolic imbalances.[8] However, increasing IOP experimentally can lead to glaucoma and, therefore, increased IOP may be sufficient, but not necessary, for induction of glaucoma.

A predominant form of this disorder is primary open-angle glaucoma (POAG), characterized by a slow increase in IOP without attendant symptoms during the early stages. By the time an individual is aware of a problem with vision, many ganglion cells have already died, and the lost vision cannot be restored. A major mechanism contributing to the death of ganglion cells in POAG is thought to be strangulation of their axons at the optic disc. The associated increased IOP is thought to produce shear forces in the tissues of the lamina cribrosa, obstructing the to-and-fro transport between the axon terminal and ganglion cell soma and leading to the death of the cell.[9–11] Clinical intervention cannot restore lost vision. It can only slow or prevent subsequent death of ganglion cells by reducing IOP. The ganglion cell axons first affected are those entering the dorsal and ventral aspect of the optic disc—those serving the peripheral nasal visual hemifield projecting on the temporal retina. Therefore, the loss of these ganglion cells (which also happen to be some of the largest) creates a characteristic crescent scotoma pattern, beginning in the peripheral nasal hemifield and progressing toward central vision.[4,12]

The macaque monkey has been used as a basic research model for studying the neural effects of glaucoma. Argon laser application to the trabecular meshwork has been used to reduce aqueous humor outflow, thereby elevating the IOP and leading to an experimental approximation of POAG.[13] Several studies have used the monkey model to describe the functional and anatomic changes that occur within the eye and optic nerve, in an effort to understand the sequelae to elevated IOP. For example, Quigley et al.[14] and Glovinsky et al.[15,16] have presented evidence that there is an early selective effect on the largest ganglion cells of the retina. These large ganglion cells purportedly comprise the magno (M)-cellular division of the geniculocortical projection. By measurements of the diameters of remaining ganglion cell axons in the optic nerve, they

From the [1]Department of Ophthalmology and Visual Science, University of Texas Medical School at Houston; and the [2]College of Optometry, University of Houston.

Supported by National Institutes of Health Grants EY-001120, EY-10608, EY07751, and EY11545; Research to Prevent Blindness; and Alcon Laboratories, Inc., Fort Worth, Texas.

Submitted for publication July 20, 1999; revised December 22, 1999; accepted January 26, 2000.

Commercial relationships policy: N.

Corresponding author: Morris L. J. Crawford, 6431 Fannin, Suite 7.024, Houston, TX 77030. crawford@eye.med.uth.tmc.edu

reported that the largest neurons are first affected (and first to die).[6,16] This conclusion stimulated the search for an early diagnostic test for glaucoma based on stimulus characteristics thought to best stimulate the M-cellular pathway. However, in an earlier study, we found no differential effect of elevated IOP on either the encounter rate or receptive field characteristics of the parvo (P)- or M-cellular lateral geniculate neurons,[17] and Vickers et al.[18] have shown that metabolism in both divisions of the afferent pathway is reduced in experimental glaucoma.

In this study we examined the effects of elevated monocular IOP on the metabolism of the P- and M-cellular divisions of the lateral geniculate nucleus (LGN) and in the primary V1 visual cortex, using cytochrome oxidase reactivity (COR) as an indicator of the visual afference from ganglion cells.[19] Cytochrome oxidase (CO) is a mitochondrial membrane protein essential for brain oxidative metabolism. It catalyzes the last step in the formation of adenosine triphosphate (ATP), the energy source for neuronal function.[20,21] The brain tissue content of CO is inhomogeneously distributed[22–24] and varies with the metabolic demand attendant to neuronal activation.[25–30] In the afferent visual system of primates, histochemistry has shown that COR decreases monotonically with the duration of sensory visual deprivation caused by enucleation or by tetrodotoxin (TTX) blockade.[31] Therefore, COR varies with the level of activation of cells in the LGN and V1 cortex and serves as a functional correlate of the surviving ganglion cells in glaucoma.

An abstract of these results has been presented elsewhere.[32]

Materials and Methods

Subjects

Twenty adult macaque monkeys (16 *Macaca mulatta* and 4 *M. fascicularis*) were used in accordance with the Office of Protection from Research Risks Public Health Service Policy on Humane Care and Use of Laboratory Animals (revised, 1986) and the ARVO Statement for the Use of Animals in Ophthalmic and Vision Research, and all research protocols had the approval of the University of Texas at Houston's Institutional Animal Care and Use Committee. The IOP of the right eye of each subject was elevated by laser application to the trabecular meshwork, using the procedures described by Quigley and Hohman.[13] The monkeys were anesthetized with ketamine hydrochloride (20 mg/kg and 0.2 mg/kg acepromazine intramuscularly), and a topical anesthetic (0.5% proparacaine HCl) was applied to the experimental eye. The trabecular meshwork was viewed through a single-mirror goniolens designed for an adult monkey's eye (Ocular Instruments, Bellevue, WA). Treatment spots were made with an argon laser operated in the blue-green mode at the following settings: spot size, 50 μm; duration, 0.5 seconds; power, 1.0 W. In the first laser session, between 60 and 100 treatment spots were made over 270° of the midtrabecular meshwork. Subsequently, IOPs were measured in the anesthetized subjects by handheld applanation tonometer, usually at weekly intervals, for a period of approximately 1 year. In some cases, the trabecular meshwork was treated additional times to produce a higher IOP. When necessary, subsequent laser exposures were conducted between 5 and 8 weeks after the initial laser surgery and involved placing approximately 30 treatment spots over the remaining 90° of the trabecular meshwork and re-treating other areas. The animals had clear ocular media throughout.

Table 1 summarizes the experimental treatments and consequent degree and duration of the resultant IOP for the monkey subjects. Subjects OHT5 through OHT24 were *M. mulatta*, which has been described and reported in an earlier article on IOP and visual field defects.[33] Subjects OHT2 and OHT3 were *M. fascicularis* reported in an earlier study on color vision anomalies after induction of experimental glaucoma[34] and two

Table 1. Macaques Used in Experiments on Monocular Experimental Glaucoma

Subject	Age (y/mo)	Laser Procedures	Laser Lesions	Highest IOP (mm Hg)	Mean Elevated IOP (mm Hg)*	Mean Control IOP (mm Hg)†
OHT2‡	Adult	1	150	67	32	14
OHT3‡	Adult	1	150	57	33	16
OHT5	6/1	3	300	52	34.9/12.0	11.5/2.3
OHT7	6/3	7	565	60§	37.0/18.2	19.7/4.8
OHT8	7/10	3	213	55	33.5/17.2	12.5/1.7
OHT9	7/9	3	170	60§	38.8/16.4	13.9/2.2
OHT11	7/0	3	188	48	40.8/5.9	11.6/1.1
OHT14	8/1	2	91	60§	49.0/13.8	16.0/2.8
OHT16	6/4	2	122	51	36.0/16.1	14.8/2.8
OHT17	8/4	1	135	46	34.3/10.1	17.1/2.4
OHT18	8/2	2	227	41	28.4/10.9	13.5/2.5
OHT19	9/2	1	103	53	37.1/13.8	17.0/2.8
OHT20	8/2	2	219	56	31.7/16.8	18.8/3.4
OHT21	6/3	2	193	43	35.4/12.7	15.6/1.7
OHT22	8/1	2	167	56	50.3/5.1	14.1/3.2
OHT23	6/3	2	149	60§	44.4/14.8	14.2/3.3
OHT24	5/4	2	168	60§	51.9/19.2	17.2/3.6
M165	Adult	1	?	52	27.5/11.3	16
M167	Adult	1	?	51	23.7/13.2	23

OHT, ocular hypertension.

* IOP of the experimental eye (mean ± SD) starting with the initial elevation of pressure.

† IOP of the control eye (mean ± SD) for the entire experiment.

‡ *M. fascicularis* Ss from Kalloniatis et al.[34]

§ An IOP of 60 mm Hg represents the scale limit for the applanation tonometer.

TABLE 2. Relative Percentage Reduction in COR in LGN Layers with Input from the Glaucomatous Eye

Field Loss	Subject	R5:6*	R3:4	R2:1	L6:5	L4:3	L1:2
1†	OHT19	4	8	7	4	9	3
2†	OHT24	4	20	11	8	10	1
3	OHT17	27	28	27	17	14	1
5	OHT23	34	28	30	29	28	4
5‡	OHT23	28	22	13	8	8	1
7	OHT16	12	15	14	3	2	1
8†	OHT18	12	10	13	8	10	6
9†	OHT20	16	10	17	11	14	10
10	OHT09	8	8	6	7	2	1
11	OHT21	11	10	13	7	9	4
12†	OHT14	14	14	15	10	6	4
13†	OHT22	22	18	20	14	25	10
Mean ± SD		15.6 ± 9.4	15.8 ± 7.0	15.5 ± 6.8	9.8 ± 7.2	10.8 ± 7.9	3.8 ± 3.2

$n = 12$.

* Column headings represent layers of the right (R) and left (L) LGN.

† Subjects described in Figure 6.

‡ Sample from central vision.

other *M. fascicularis*, M165 and M167, were subjects reported in an earlier publication on electrophysiology of ganglion cell input to the LGN after experimentally induced glaucoma.[17]

Behavioral Perimetry and Electrophysiology

For several months before and after the elevation of IOP in the right eye, the monkeys were trained and tested for visual field threshold sensitivity using behavioral methods and a visual field analyzer (model 630; Humphrey Allergan, San Leandro, CA). The full details of these testing procedures and the extent of the visual field defects have been published elsewhere.[12,33] The resultant visual field maps (VFMs) were ranked for severity of defect by five practicing ophthalmologists, and the average of the rankings for each animal was used to classify the visual defect as mild, moderate, or severe (Table 2). At the end of the visual field threshold sensitivity testing, many of the animals were used in a terminal electrophysiological study, in which the relative responsiveness of the cells in the P- and M-cellular LGN divisions was compared. The objectives and methodology of these experiments have been described earlier.[17]

Tissue Preparation

At the end of the behavioral or electrophysiological study, the animals were overdosed with 100 mg/kg pentobarbital sodium (Nembutal; Abbott, Abbott Park, IL), exsanguinated by 2 l saline, followed by 2 l 2% paraformaldehyde-0.5% glutaraldehyde fixative in phosphate buffer (pH = 7.4). The brain and optic nerves were removed, and (in most cases) the visual cortices were dissected and gently flattened on a glass slide. The tissue was refrigerated overnight in the fixative before it was subjected to a sucrose dehydration gradient of 10%, 20%, and 30%. The thalamus containing both LGNs was blocked for coronal section and dehydrated in a similar manner. The tissue blocks were embedded in compound (TissueTek; Miles, Elkhart, IN) and frozen in liquid nitrogen–cooled acetone. The visual cortices were sectioned at 30-μm thickness tangential to the cortical surface, and the LGNs were sectioned in a similar thickness in the coronal plane. Serial sections were treated for the histochemical localization of CO, according to the protocol of Wong–Riley.[19] The CO-stained sections were mounted on gelatinized slides, dehydrated, and coverslipped in Permount (Fisher, Fair Lawn, NJ).

Optical Measurements

The relative CO content and distribution in brain tissue was inferred from the relative histochemical COR on the assumption that the higher the density of the COR product, the higher the CO content in the tissue. A reduction in COR in the brain tissue connected with the experimental eye was defined relative to the COR in the adjacent tissue connected with the normal companion eye in the same tissue section and was interpreted as a reduction in afferent stimulation from retinal ganglion cells in the experimental eye. COR was measured in the layers of the LGN and in the input layer of layer 4C of the V1 cortex by image analysis software (ImagePro Plus; Media Cybernetics, Silver Spring, MD). The stained sections were homogeneously back illuminated, imaged with a CCD camera (Sony, Tokyo, Japan) and displayed on a monitor (NEC, Tokyo, Japan), captured, and scaled 0 to 255, where 0 is opacity and 255 is the incident light. All measurements were taken before any filtering or contrast enhancement of the image. $COR = I - T$, where I is the incident light (nominally a value of 255), and T is the light transmitted through the tissue containing the COR product. The value of COR from tissue connected with the experimental eye (COR_G) was always compared, in the same section, with the value of comparable COR in the adjacent companion area (LGN layer or V1 ocular dominance column; ODC) having input from the normal eye (COR_N). The ratio COR_G–COR_N constituted the primary data from which mean values and variances were calculated. Normally, the mean COR ± SD of a standard 400-pixel array was recorded at each tissue site, and the ratio of COR_G to COR_N formed. A minimum of 10 such ratios were then averaged for each tissue location. Most often, the ratio COR_G–COR_N was expressed as a percentage reduction of COR, relative to that in the companion site that had input from the normal eye.

The relative COR measurements were imported into a spreadsheet (QuattroPro; Corel, Ottawa, Ontario, Canada) for computation and graphing, and the paired *t*-test and Mann–

Whitney rank sum test were applied using SigmaSTAT (Jandel Scientific, Corte Madera, CA).

RESULTS

Glaucoma and the LGN

The typical pattern and distribution of COR for normal and glaucomatous LGN are illustrated in the digitized and contrast-enhanced images of Figures 1 and 2. The dark COR product is illustrated in Figure 1A in a coronal section through the caudal one third of the right LGN of a normal adult monkey. All six layers of the nucleus are shown, and an approximate representation of the horizontal meridian (HM) for the contralateral hemifield is indicated by the transecting line.[35] The measurements of COR were taken near the representation of the HM (Fig 1. open squares in each layer), a locus generally found to show an early defect using the Humphrey VFM (see Fig. 6). The actual size, shape, and location of the sample area where the COR product density was measured varied somewhat within the layer to avoid artifacts associated with histologic mounting (e.g., folds, wrinkles, and tissue debris). Most often, the change in location was made to avoid the large blood vessels that penetrate the LGN (e.g., Fig. 1A, arrow). With this reservation, an effort was made to sample, as close as possible, the same representation of visual space across all LGN layers.

For assurance that the reduction in LGN metabolism after different degrees of experimental glaucoma was dependent on afference from retinal ganglion cells, we measured and compared the COR changes in a monkey that had monocular injection of TTX into the LGN for blockade of the ganglion cells.[27] Figure 1B illustrates the contralateral left LGN of a monkey after 3 weeks of ganglion cell blockade by intravitreal TTX injections sufficient to maintain a complete blockade of the flash-evoked cortical potential. The reduction in COR was

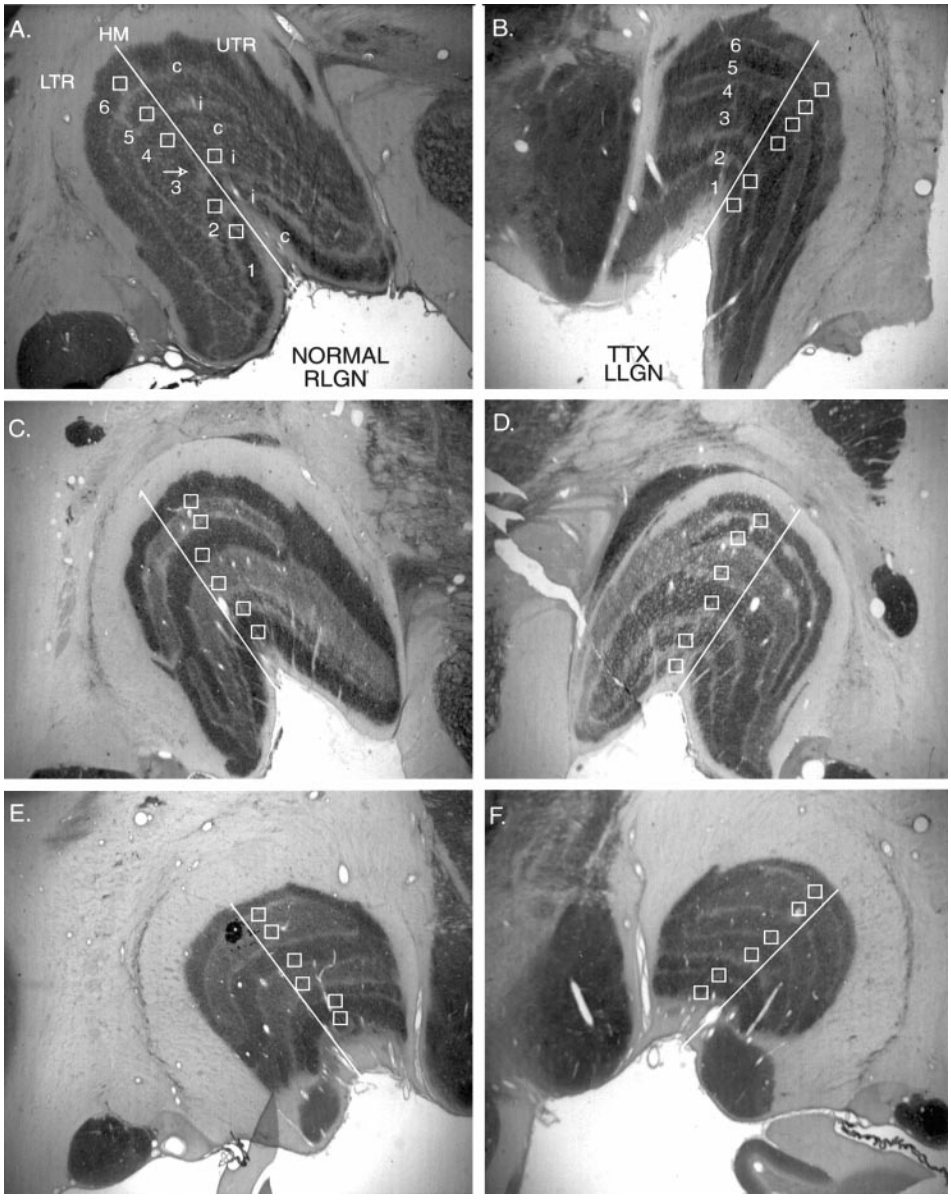

FIGURE 1. COR in the LGNs of macaques (*M. mulatta*). (**A**) Normal monkey LGN with the central line approximating the horizontal meridian (HM) of the visual hemifield. *Squares:* typical loci where COR was measured. LTR, lower temporal retina; UTR, upper temporal retina. Layers are numbered, and the inputs from the ipsilateral and contralateral eye are indicated. *Arrow:* penetrating blood vessel. (**B**) LGN of monkey after 3 weeks of continuous TTX blockade of the contralateral right eye. Reduction in COR is evident in layers 1, 4, and 6 relative to the normal eye input to layers 2, 3, and 5. (**C**) LGN section representing the midperiphery of the visual hemifield from a monkey with long-standing glaucoma of the ipsilateral right eye, showing COR reductions in layers 2, 3, and 5. (**D**) Contralateral LGN of the same monkey, showing that the contrast in COR is less than that seen in the ipsilateral LGN. (**E**) LGN section recipient of central vision from the same monkey as in (**C**) and (**D**), indicating that the COR contrast is less than at more peripheral loci (**C**). (**F**) The COR contrast between layers in the contralateral LGN of the same monkey is very low, suggesting that the scotoma of glaucoma had not spread to fully involve the central vision. All images in this figure have been digitized and contrast enhanced for illustrative purposes only. All relative density measurements were taken before contrast enhancement; magnification, arbitrary.

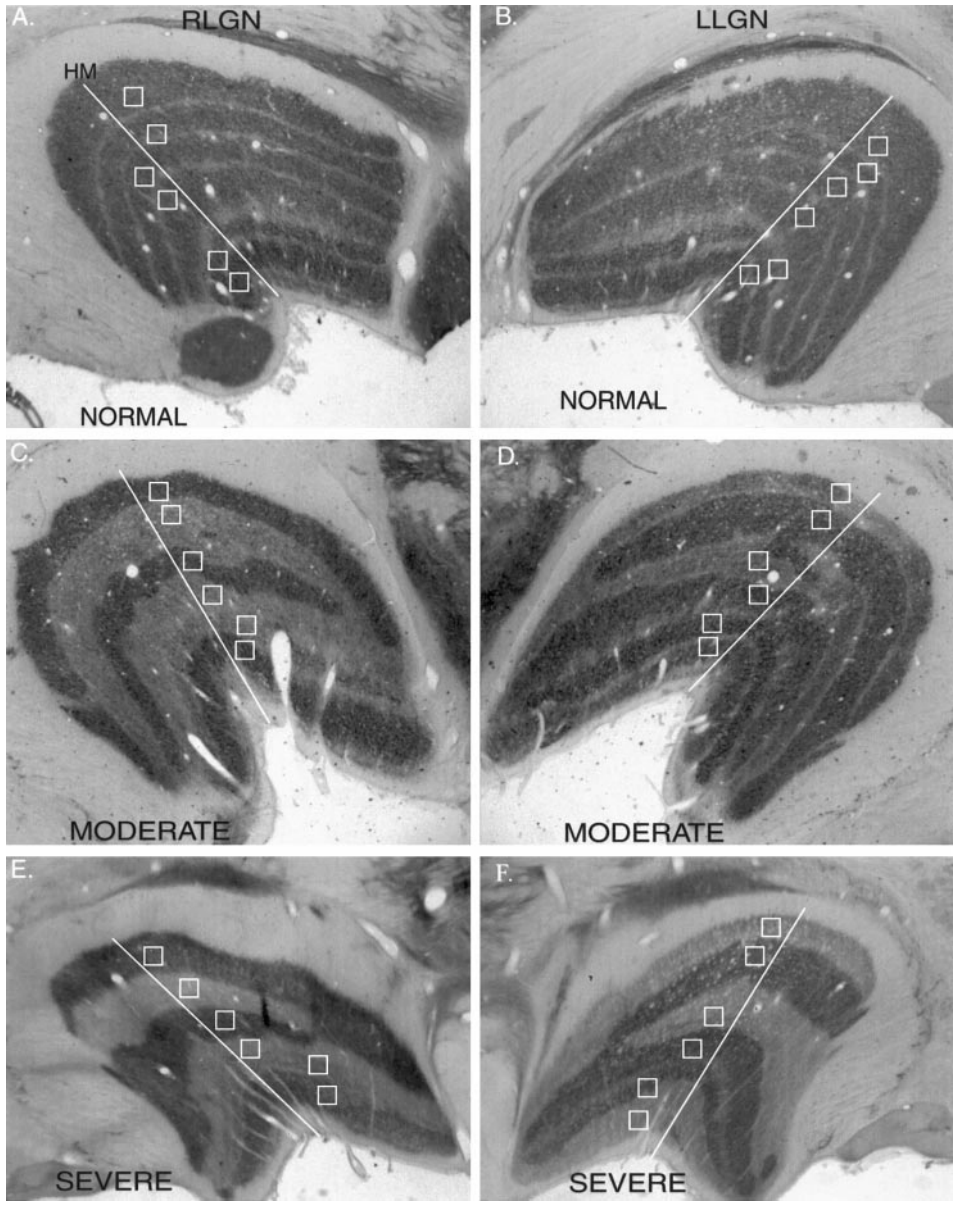

FIGURE 2. COR in the left (LLGN) and right (RLGN) LGNs of a normal monkey (**A**, **B**) compared with that seen in a monkey with moderate (**C**, **D**) and another with severe glaucoma (**E**, **F**) of the right eye. Note the increase in COR contrast in the ipsilateral RLGN between (**C**) and (**E**). The *lines* and *squares* indicate the approximate line and loci of CO density sampling. All COR relative density measurements were taken before contrast enhancement; magnification, arbitrary.

clear after TTX blockade. The relative COR in LGN layers 1, 4, and 6, which receive input from the TTX-injected right eye, was clearly less in comparison with the COR in layers 2, 3, and 5, which receive input from the normal ipsilateral left eye. Therefore, blocking afferent ganglion cell stimulation with TTX reduced the COR in the recipient LGN layers and produced a pattern identical with that seen in experimental glaucoma (see Fig. 4 for a quantitative comparison).

Figure 1C through 1F illustrates the change in COR in LGN layers with input from a glaucomatous and a normal eye (M165) as a function of position in the LGN. In Figure 1C, from the middle of the nucleus representing midperipheral vision, the right LGN shows the COR in layers 2, 3, and 5, receiving input from the ipsilateral experimental right eye, to be reduced in comparison with the COR-rich layers 1, 4, and 6, receiving input from the normal left eye. In the companion left LGN (Fig. 1D) the relative contrast in COR between layers 1, 4, and 6, receiving input from the glaucomatous contralateral right eye, and layers 2, 3, and 5, receiving input from the normal eye, was not nearly as great. This reflects the nature of the spread of the experimental retinal defect (see subsequent Fig. 6) which was typically first seen in the peripheral nasal hemifield. The temporal retina defect progressed to cross the vertical meridian and subsequently involved the nasal retina. Therefore, the contrast in COR between glaucomatous and normal LGN layers was usually lower contralateral to the experimental eye.

Figure 1E shows a section representing central vision for this same monkey. Note that the COR contrast between normal and glaucomatous layers was much less than that just described for the more peripheral retinal representation shown in Figure 1C, again suggesting that the glaucomatous retinal lesion had not spread to fully involve central vision. As was the case for the comparison between Figures 1C and 1D, the effects of experimental glaucoma are barely noticeable in Figure 1F, representing central vision in the contralateral left LGN. To summarize these data, experimental glaucoma in monkeys typ-

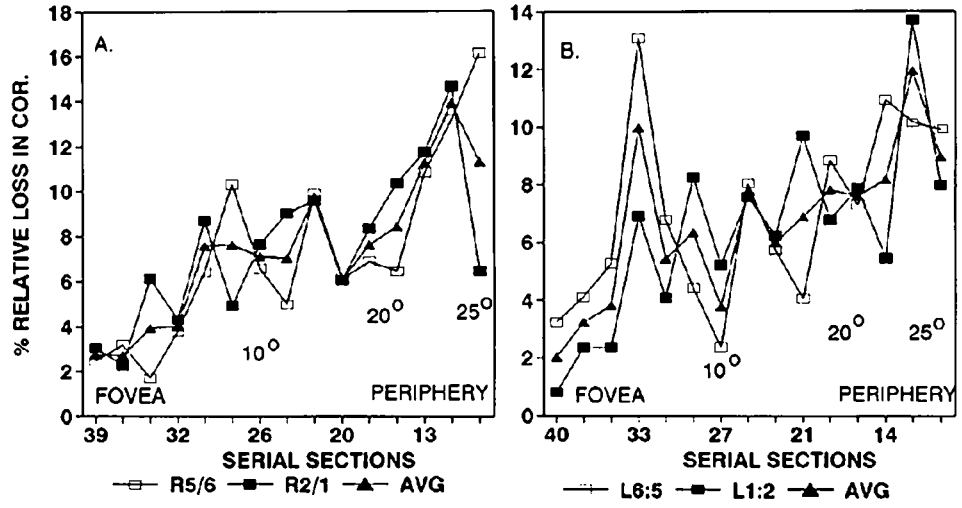

FIGURE 3. (**A**) Relative loss in COR along the representation of the HM from near the fovea into the midperiphery of the ipsilateral right LGN. Note that the COR changes approximately the same amount in the P-cell laminae (R5/6) as in the M-cell laminae (R2/1) with increasing depth of the scotoma. (**B**) The COR measurements showing the comparable relative loss in the contralateral left LGN of the same monkey (OHT8).

ically mimicked clinical glaucoma, in that the visual field defects frequently were first observed in the nasal visual field, affecting the temporal retina, which projected on the ipsilateral LGN where COR was reduced with the loss of ganglion cell afference. As the glaucomatous lesion spread over the retina to cross the vertical meridian, the effects began to appear in the contralateral left LGN.

The progressive relative reduction in COR with severity of glaucoma (judged from visual field measurements; see Fig. 7) is shown in Figure 2. Figures 2A and 2B show normal LGN sections representing the projection site of the midperipheral visual hemifields. With moderate glaucoma of approximately 1 year's duration (Fig. 2C; OHT20), ipsilateral LGN layers 2, 3, and 5 were CO poor, whereas the layers receiving input from the normal contralateral companion eye (layers 1, 4, and 6) showed robust COR. Again, in the left LGN (Fig. 2D) the contrast between relative COR in the glaucomatous and normal layers was much less, indicating the encroachment of the lesion into the nasal retina.

More severe glaucoma (Figs. 2E and 2F (OHT22) caused a further reduction of the COR in the layers connected with the glaucomatous eye. However, even with long-standing severe glaucoma, there was still some afferent input from the experimental eye, as suggested by the lower relative contrast in COR between layers with input from the glaucomatous and normal eyes in the contralateral left LGN (Fig. 2F).

The degrees of relative loss in COR within the P layers and the M layers were similar in experimental glaucoma (Fig. 3A). Fifteen serial sections along the representation of the horizontal meridian were measured for the percentage COR reduction in ipsilateral P-cell layer 5, relative to normal P-cell layer 6. In the same sections, the M-cell layers 1 and 2 were similarly compared. The serial sections extended from the foveal representation to the depth of the glaucomatous lesion at approximately 25° in the periphery. In the ipsilateral right LGN, there was a monotonic reduction in COR from 2% to 13% over this range. Importantly, there were no significant differences in COR between the P- and M-layers throughout, indicating that the M-cells were no more sensitive to ocular hypertension than were the P-cells.

Figure 3B shows the relative changes in COR at corresponding loci in the contralateral left LGN where the progressive change in COR with distance from central vision was more irregular than that seen in Figure 3A. Once again, there was no differential effect of the glaucoma between the P- and M-layers. The variation in COR in the LGNs suggests that the spread of the glaucomatous lesion over the retina is more irregular by the time it reaches the nasal retina.

Quantitative relative COR in normal LGN layers is shown in Figure 4A. The average COR for four LGNs from three

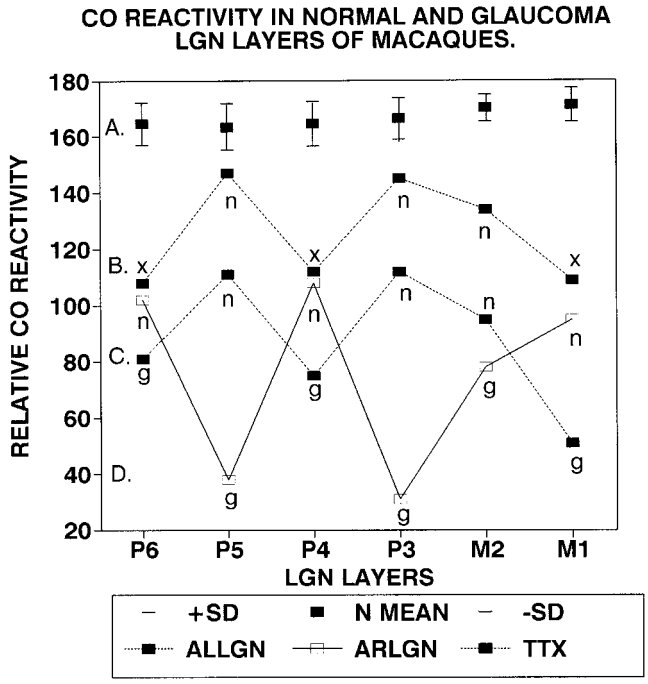

FIGURE 4. (**A**) Relative COR (mean ± SD) in the P- and M-cell laminae of four LGNs from three normal monkeys. Adjacent layers did not differ significantly in COR, nor was there a difference in relative COR between the P- and M-cell layers. (**B**) The pattern of relative COR loss was the same in layers with input from the TTX-blocked eye (x) relative to layers with input from the normal eye (n), similar to the experimental glaucoma (g) shown in (**C**). (**D**) The companion ipsilateral right LGN shows significantly greater relative COR loss in layers with input from the glaucomatous eye (g) than that seen in (**C**) showing the left LGN of the same monkey. The positions of the curves on the ordinate are arbitrary and have been separated for ease of inspection.

control monkeys is shown for comparison with LGNs from TTX-treated and glaucomatous monkeys (Figs. 4B, 4C, 4D). In four normal LGNs, adjacent layers were not significantly different in COR: The average relative difference between adjacent layers was only 1.7% (P-cell layer [P]6, 144.7 ± 7.6; P5, 143.5 ± 8.1; P4, 144.7 ± 7.8; P3, 146.6 ± 7.4; M-cell layer [M] 2, 150.2 ± 4.6; M1, 151.2 ± 6.0; F = 0.81, $P < 0.55$). Of note, there were no significant differences in COR between the P- and the M-cell divisions of the nucleus (e.g., Student's *t*-test: 1.5 between M1 versus P5, the largest mean differences between M- and P-cell layers, $P < 0.18$, not significant). This result suggests that the overall metabolic demands of neurons in the two divisions—each known to have predominant input from different ganglion cell types (smaller, β-type ganglion cell input to neurons in the P-cell layers; larger, α-type ganglion cell input to neurons in the M-cell layers)—are normally the same.

Figure 4B shows the quantification and comparison of the pattern of relative loss in COR in the contralateral left LGN after 3 weeks of TTX blockade, with Figure 4C showing a monkey after induction of experimental glaucoma. The pattern and magnitude of average COR loss (Fig. 4, x) after complete TTX blockade of 3 weeks' duration was virtually identical with that seen with a moderate level of glaucoma (Fig. 4, g). This result argues that it is the loss of ganglion cell afference that leads to the reduction in COR in the LGN. Although the pattern (and in this case, the magnitude) of relative change may be the same, the magnitude of the change with experimental glaucoma may be considerably greater, as illustrated in Figure 4D. As was typical for all the results, the relative loss (Fig. 4, g) in layers 1, 4, and 6 of the contralateral left LGN was 19%, 23%, and 27%, respectively, whereas the relative loss in glaucoma-affected layers in the ipsilateral right LGN was much greater, at 63%, 71%, and 17% less than normal (Fig. 4, n).

Table 2 summarizes the percentage of relative loss in COR in the LGNs of 12 monkeys for which we had both visual field measurements and complete COR measurements in both LGNs. The monkeys are arranged in the table based on increasing severity of loss in the VFM (see the Methods section and Fig. 6). Table 2 shows that the average reduction in COR was virtually identical at 15% for both the P- and M-cell layers of the ipsilateral right LGN. From these results, it is clear that experimental glaucoma did not have a selective and more detrimental effect on the M-cell pathway. However, in the contralateral left LGN, the reduction in COR was significantly less, with the least detrimental effect seen in the M-cell layers.

When the data from the other monkeys (many showing the more severe effect illustrated in Figs. 6E and 6F) were added to include all 20 monkeys, the pattern of loss remained essentially the same, whereas the degree of COR loss increased. Figure 5 graphs the average loss in COR in the LGNs of all monkeys. As would be expected, the average percentage reduction in COR was significantly greater in the ipsilateral layers of the right LGN (22%) than in the contralateral left LGN (13%; $t = 3.67$; $df = 17$; $P < 0.001$). This reflects the characteristic progression of the glaucomatous lesion, beginning in the temporal retina and spreading into the nasal retina. The percentage loss in the ipsilateral P-cell layers 5 and 6 was significantly greater (24%) than the loss in the ipsilateral M-cell layers 2 and 1 (20%; $t = 2.51$; $P < 0.05$), suggesting that glaucoma had a greater effect on the metabolism of the P-cells than on the M-cell system.

The VFM and COR

To show the general association between the degree of visual field loss indicated in the Humphrey VFM, the reduction in COR in the LGN, and the input to the V1 cortex, the data from six monkeys are presented graphically in Figure 6. Figure 6A shows the VFM of the experimental right eye of OHT24, judged to be one of the least affected of the experimental monkeys. Although there was no apparent gross defect in the VFM, there were a substantial reduction in COR in the recipient layers of the ipsilateral LGN, shown in the histogram for the ipsilateral right LGN. The P-cell layers 5 and 3 showed a reduction of 4% and 20%, respectively, whereas the M-cell layer 2 showed a robust 11% reduction. The average reduction in the P-cell layers of 12% was comparable to the 11% reduction in the M-cell layer. The histogram also shows that as the COR reduction occurred in the LGN, there was a concurrent small reduction in COR evident in the input layer 4C of V1 cortex. The data on the V1 cortex will be discussed in more detail later in the article.

Figure 6B shows the VFM of another monkey, OHT19, judged from the VFM in a way similar to OHT24 to have minimal sensitivity loss. However, the histogram for the ipsilateral right LGN shows that the reduction in COR was substantial, with the P-cell layers 5 and 3 showing a 4% and 8% reduction, respectively. The reduction of 7% in the M-cell layer was comparable to the average P-cell layer reduction of 6%. The histogram data to the right shows that these significant LGN reductions in COR were reflected in metabolic reductions in the respective input layer 4C sublayers of V1 cortex.

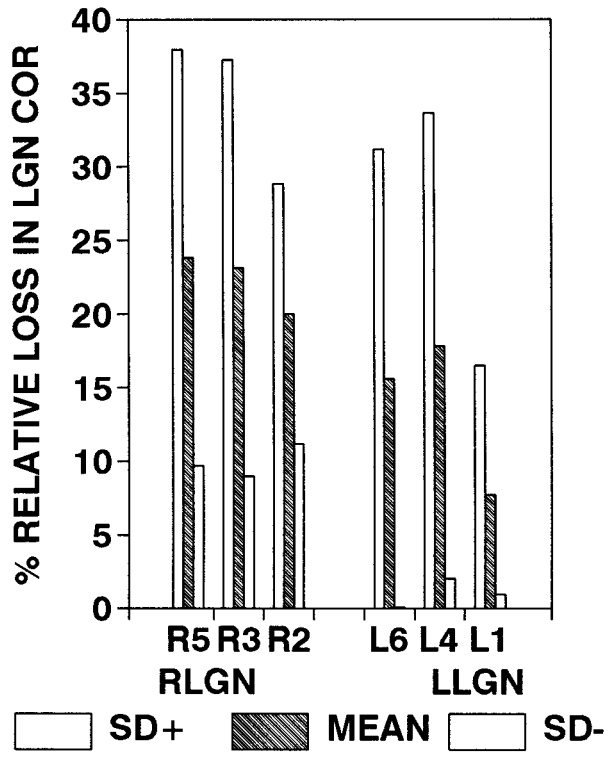

FIGURE 5. Relative COR losses in the ipsilateral right LGN (RLGN) and the contralateral left LGN (LLGN) of 20 monkeys with experimentally induced glaucoma of the right eye. The losses in COR were greater in the ipsilateral RLGN, with the smallest effect in the contralateral M-cell layers.

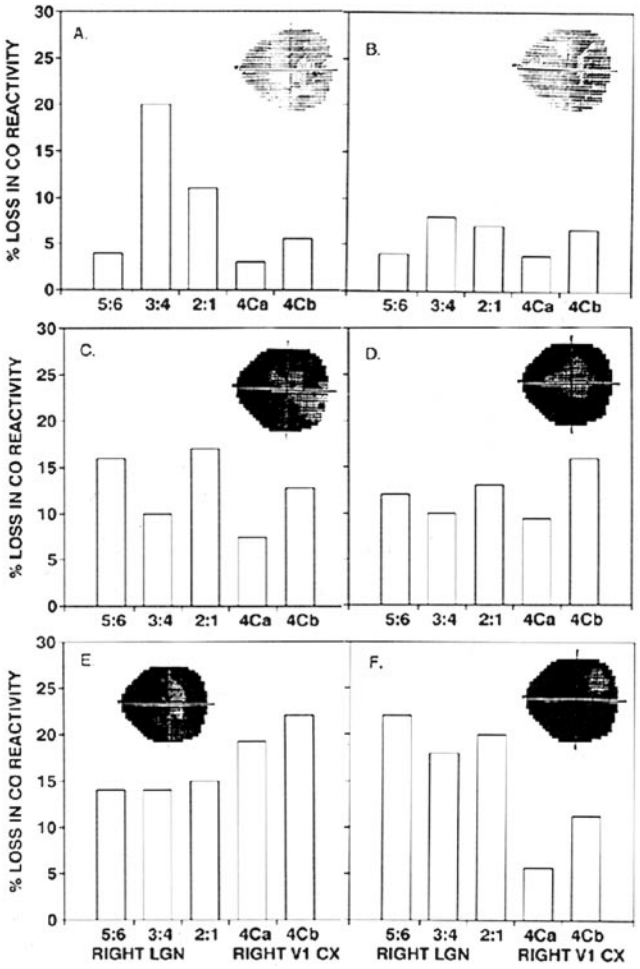

Figure 6. *Insets* show VFM of the glaucomatous right eye of monkeys. Histograms show relative loss in COR in the ipsilateral right LGN, M-cell recipient layer 4Cα, and P-cell recipient layer 4Cβ of the ipsilateral V1 cortex. Monkeys OHT24 (**A**) and OHT19 (**B**), judged to have mild glaucoma; monkeys OHT20 (**C**) and OHT18 (**D**), judged to have moderate visual field loss; monkeys OHT14 (**E**) and OHT22 (**F**), judged to have severe glaucomatous visual field defects.

Taken together, these two examples show that by the time a defect became evident in the VFM, substantial effects of glaucoma could be seen in the COR of the downstream pathways. This is in agreement with the relationship we have described recently between the loss of ganglion cells and the VFM, in which more than half the ganglion cells of the macaque retina are lost by the time a sensitivity loss can be detected in the VFM.[36]

Figure 6C shows the VFM of subject OHT20, a monkey that was judged to have a moderate loss in visual field sensitivity, based on the size, location, and depth of the defect. Correspondingly, the histogram for the right LGN shows that the loss in COR in the P-cell layers of the LGN was increased to an average 13%, whereas the M-cell layer had a slightly and insignificantly larger 17% loss. Compared with the previous examples (Figs. 6A, 6B), there was a greater loss in COR of approximately 10% in the input layers of V1 cortex.

The VFM of subject OHT18, another monkey judged to have a moderate loss in sensitivity, is shown in Figure 6D. Comparable to the effects seen in OHT20, the histogram shows that the P-cell layers of the LGN lost an average of 11% in COR, whereas the M-cell layer lost 13%. The relay of these effects to the V1 cortex, again seen to the right of the figure, indicate that there was an overall loss of 12% in COR.

Judged to have relatively moderate losses according to the VFMs, these two monkeys showed a greater average LGN reduction in COR of 12% compared with the average 8% reduction seen in the two examples judged to have mild losses. Correspondingly, these greater reductions of COR in LGN were relayed to the V1 cortex.

Figures 6E and 6F are the VFMs of monkeys OHT14 and OHT22, respectively. These monkeys were judged to have a severe loss in sensitivity. In these monkeys, both the P- and the M-cell layers of the LGN showed approximately a 14% to 20% reduction in COR, with the relay of these effects to the V1 cortex manifesting losses of 7% and 20%, respectively.

These latter two relatively severe cases of VFM defect show the greatest average reduction in LGN COR of 17%, compared with 12% for the two moderate cases and the 8% found in the mild cases. In short, there was a monotonic increase in the loss in COR within the LGN and the V1 cortex with the degree of severity of the VFM defect. Figure 7 summarizes the average relationship between the COR (mean $\pm$ SD of the five measurement sites in LGN and V1) and the VFM for these six monkeys. The mild stage of glaucoma was significantly different from both the moderate and the severe levels of glaucoma (analysis of variance; $F = 6.1$, $P < 0.006$), whereas there was no difference between the moderate and severe levels.

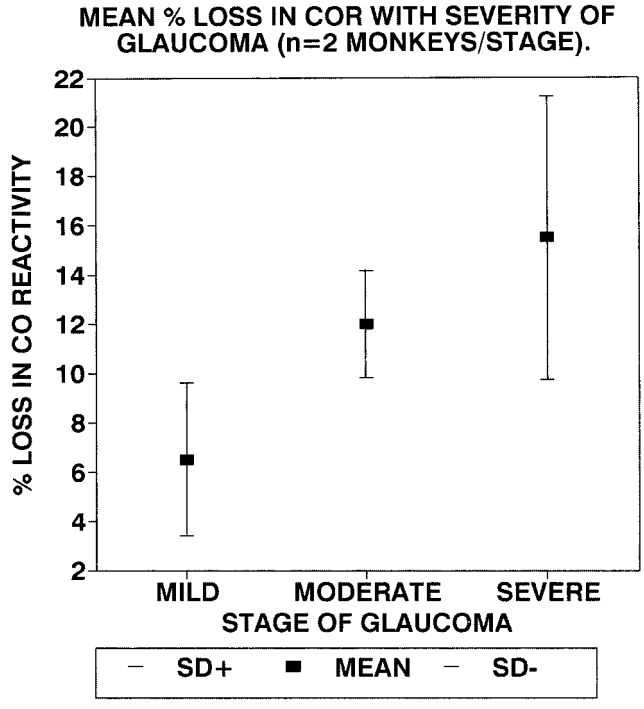

Figure 7. A summary of the progressive loss in COR associated with the mild, moderate, and severe visual field defects of the six monkeys described in Figure 6. Means $\pm$ SD for loss in COR in five sample sites (right LGN layers 5, 3, and 2 and V1 layers 4Cα and 4Cβ) for two monkeys.

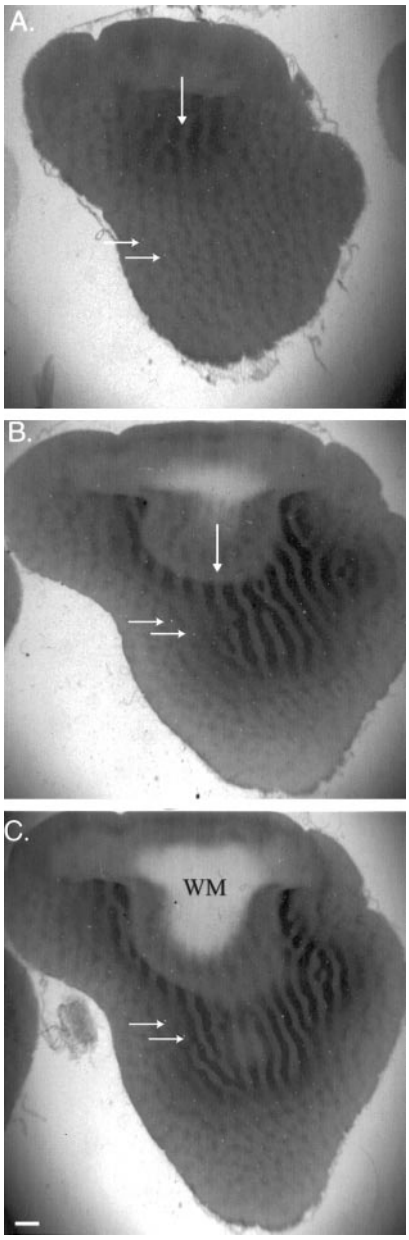

FIGURE 8. Tangential serial sections stained for COR through the ipsilateral V1 cortex of a monkey with experimental glaucoma of the right eye. *Vertical arrow:* CO-rich ODC in layer 4C, which has input from the normal left eye. The adjacent CO-poor ODC has input from the glaucomatous right eye. *Horizontal arrows:* same blood vessels, which could serve as fiducial alignment marks. The alternating rows of CO-rich blobs in layers 2 and 3, which lie directly above the ODC of layer 4C, can be seen in (**A**). WM, white matter. Bar, 1 mm.

Glaucoma and V1 Cortex

With experimental glaucoma, afferent input to the primary V1 visual cortex is dramatically altered consequent to the changes in LGN. We next describe the details of these effects. Figure 8 is a tangential view of three serial CO-stained sections from the posterior bank of the lunate sulcus (A) extending into the cortical representation of the lower visual field of paracentral vision (C) from a monkey with glaucoma. CO-rich layer 4C ODCs, receiving input from the normal left eye (vertical white arrows), and the adjacent CO-poor ODCs, receiving input from the glaucomatous right eye, are seen clearly. As would be expected in adult monkeys, the widths of the columns were about the same,[37] differing only in COR, which varied between animals depending on the cortical location of the representation of the visual hemifield and on the severity of the glaucomatous condition. Owing to the cortical curvature in this nonflattened cortex, the CO-rich ODC of layer 4C (Fig. 8A, white vertical arrow) was seen in subsequent sections to lead to the rows of interconnected CO-blobs that overlay layers 2 and 3. In a similar manner, the adjacent CO-poor layer 4C ODC, receiving input from the glaucomatous eye, led to a row of smaller CO-blobs, a row of blobs that had no interconnecting COR. The horizontal arrows indicate a pair of blood vessels in each section, which served as fiducial marks for alignment of the three images.

Figure 9 presents a coronal view of monkey V1 cortex. Each of the three panels shows a Nissl-stained section matched

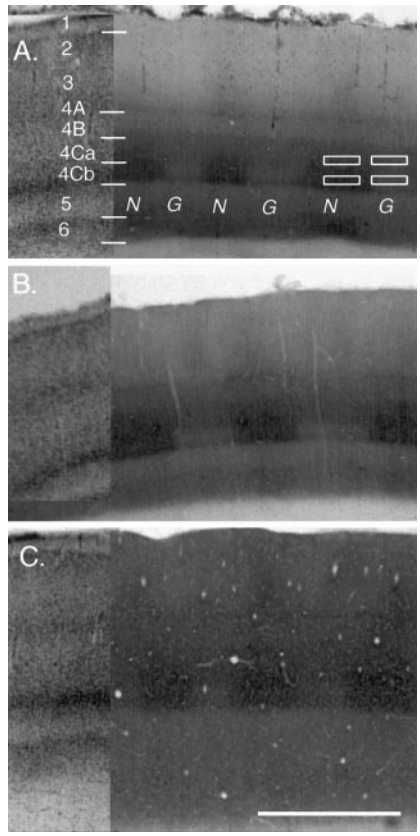

FIGURE 9. A coronal view of the V1 cortex of three monkeys which had experimentally induced glaucoma in the right eye. Nissl-stained sections have been matched to sections stained for COR. The Nissl-stained layers are labeled, whereas the adjacent CO-stained sections from (**A**) a monkey with moderate glaucoma, (**B**) a monkey with severe glaucoma, and (**C**) a monkey with mild glaucoma, show the CO-rich ODC with input from the normal left eye (N) next to the CO-poor ODC with input from the glaucomatous (G) right eye. Evident are the two zones of COR in the left eye ODC, layer 4C, with the *bottom* portion appearing much lighter than the *top* portion. The rectangles represent approximate sample areas for measurement of COR in the P- and M-cell recipient zones. In (**B**) the CO pale rectangular zone representing input to the P-cell recipient zone is even more clearly defined. (**C**) Though less distinct, the pattern of COR is evident, even in mild glaucoma. Bar, 1 mm.

to a CO-stained section. The well-known six layers of V1 are labeled in Fig. 9A, which shows cortex from a monkey with moderate experimental glaucoma of the right eye. The CO-poor columns (G) are shown, and the CO-rich columns (N) are associated with input from the normal left eye. Inspection of the glaucomatous CO-poor columns reveals a difference in COR in the two afferent input subdivisions of layer 4C; the lower portion of layer 4Cβ is seen as a pale rectangular zone, whereas the upper layer 4Cα sublamina is seen to be considerably darker. Figure 9B shows the same phenomenon for another glaucomatous monkey, whereas Figure 9C shows that this differential effect on the COR in these two V1 input divisions could be seen after only a few months of experimental glaucoma. The horizontal rectangles in Figure 9A indicate the loci where COR was measured and the differential loss in COR computed in all the monkeys.

Figure 10 shows the pattern of loss in COR for the M-cell (4Cα) and for the P-cell (4Cβ) input divisions to V1 cortex. The mean percentage loss ($\pm$1 SD) in COR for 10 samples each is shown for the 17 monkeys for which complete measurements were obtained for both V1 cortices (in some of the mild glaucoma cases, columns could not be discerned in the contralateral left cortex). The average percentage loss in relative COR in the right cortex (mean R4Cα = 8.1%, mean R4Cβ = 13.8%; $t = 9.1$; $P < 0.0001$) was nearly the same in the left cortex (mean L4Cα = 8.3%, mean L4Cβ = 14.9%; $t = 7.2$; $P < 0.0001$). In both cortices, the reduction in relative COR was significantly less in the M- than in the P-cellular input sublamina. In every monkey, the relative COR loss was significantly less in the M-cell input layer than in the P-cell input layer. On average, the loss was 8% in the 4Cα layer and almost double that at 14% in the 4Cβ sublayer.

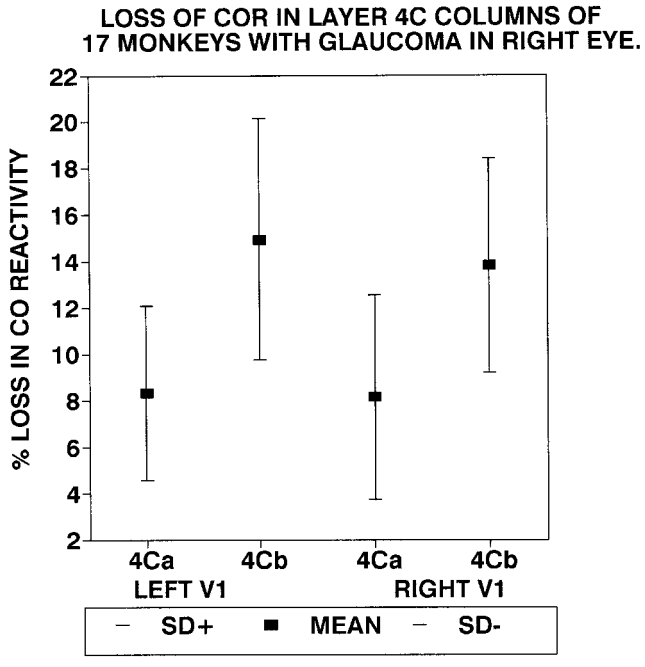

Figure 10. The average ($\pm$ SD) relative loss in COR in the M-cell (layer 4Cα) and in the P-cell (layer 4Cβ) of the 17 monkeys for which COR was sampled in both V1 cortices. In all 17 cases, the loss was significantly greater in the P-cell recipient zones, as reflected in the summary group data.

The results of these experiments examining the relative changes in visual afference with experimental glaucoma may be summarized as follows: Experimental glaucoma reduced COR in both the P-cell and the M-cell divisions of the LGN, with a somewhat greater reduction in the P-cell division, reduced the COR significantly more in the P-cell input to V1 layer 4Cβ than in the M-cell layer 4Cα, created a CO lesion first in the ipsilateral visual brain representing the nasal visual hemifield of the glaucomatous eye, and then progressed to the contralateral visual brain as the retinal scotoma enlarged.

Discussion

A primary reason for the assessment of the effects of experimental glaucoma on the visual brain was the proposal that the disorder has a differential detrimental effect on the two major afferent divisions, the P- and the M-cell pathways. Quigley et al.[13–16] have presented results showing an early, more severe, effect of glaucoma on the larger ganglion cells, presumed to be predominantly the Pα ganglion cells of the M-pathway, rather than the Pβ ganglion cells. However, Johnson[38] has reinterpreted the data of Quigley et al.[39] and suggested that the original data show, at best, a modest trend for a selective early loss in large-diameter axons—that is, in the M-pathway. Although we have yet to measure the actual differential loss in different sizes of ganglion cells, the results of our metabolic study of the downstream brain targets in monkeys with mild visual field defects are not consonant with the idea that glaucoma has a more detrimental early effect on neurons in the M-cell pathway. Vickers et al.[18] have shown that experimental glaucoma in monkey affects the metabolism in both divisions of the geniculocortical afferent pathway, but they did not quantify the differences.

Beginning in the LGN, the reduction in COR within the P- and the M-cell laminae were shown in the current results to be very much the same, with the magnitude of the change being associated with the degree of the visual field defect (Figs. 6, 7). Although this association was the general finding, there were notable exceptions (Table 2, OHT23; also see Fig. 1 of Reference 36) when there were only moderate changes in the VFM but a dramatic change in COR. Although the period between the last VFM measurements and the termination of the monkey was relatively short (<2 weeks), we cannot rule out additional loss in ganglion cell function during this interval. There was a second case, however (Table 2, OHT9; also Fig. 4A in Reference 36), in which the VFM showed a severe loss in sensitivity, but the subsequent loss in COR was relatively mild. These two exceptions to the general finding of a progressive loss in COR with increasing loss in visual sensitivity had similar treatment histories (Table 1). As in clinical glaucoma, the progression of the defect in the VFM in experimental glaucoma is often variable in rate and degree of loss in sensitivity, contributing to variability in the association between COR and the VFM.

Regarding the differential effect of glaucoma on the M- over the P-ganglion cells, it could be argued that there is an early selective effect on M-cells,[15] but that our experimental series did not cover the proper period. This seems unlikely, because our series of monkeys included those with a just-detectable VFM defect to those with end-state defects, and the relative pattern of the effect on the two pathways remained the same. In addition, the pattern of the spread of the glaucoma-

tous lesion over the retina was such that it finally involved input to the contralateral brain structures, where any preferential detrimental effect on the M-cell targets would be expected to show up. On the contrary, the greater reduction in COR was instead seen in the P-cell projection sites (Table 2 and Fig. 9). These collective data show that experimental glaucoma has a greater impact on the metabolism of the P-cell pathway in both the LGN (Fig. 5) and especially in the input layer 4Cβ of the V1 cortex (Figs. 9, 10). In every monkey, the COR reduction in the layer 4Cβ was significantly greater than that in the companion input layer 4Cα, the recipient zone for the M-cell input from the LGN. Because the afference to these sublaminae is dependent on the LGN input,[40] this difference in COR may well reflect what is relayed to V1 from the LGN. In short, the COR in the LGN showed a greater effect of glaucoma on the P-cell pathway than on the M-cell pathway, and these differences were relayed and exacerbated in the corresponding COR in the layer 4C sublaminae.

By the time there is a detectable defect in the VFM, more than half the ganglion cells have died.[36] Therefore, the standard VFM cannot be used for the detection of the earliest vulnerability of ganglion cells in glaucoma. It may well be that by the time the retinal defect has progressed to the point of a detectable VFM defect, any initial differences that glaucoma had on the two afferent pathways may have been obliterated. Weber et al.[41] examined the issue of greater differential effects of experimental glaucoma on the morphology of parasol (M-cells) and midget (P-cells) ganglion cells. Although they found no substantial differences in the soma size between ganglion cell class with progression of the disease, there were qualitative differences in the size and complexity of M-cell dendritic arbors earlier in the disease. This finding is consistent with an initial degenerative effect beginning with the M-cells and is consonant with the results of Glovinsky et al.[15] The mechanism of this early period in ganglion cell death deserves more investigation, and a search should be made for a more sensitive method for the early detection of glaucoma.

The precipitating event for these metabolic changes in the LGN and V1 cortex is the functional impairment or death of retinal ganglion cells. Functional blockade by TTX is shown to be sufficient to reduce COR in the afferent recipient zones of the LGN and V1, in a pattern (if not in degree) similar to enucleation. However, there are important differences between the effects of TTX or enucleation and ganglion cell loss in glaucoma, experimental or clinical. TTX blockade and enucleation result in total and immediate loss of afference to downstream targets, whereas the loss from POAG is generally more gradual, progressing over a period of months to years. We cannot differentiate between the relative contributions of the death of ganglion cells or the functional impairment of ganglion cells in reduction of COR presented in the current study. However, in those cases in which we have compared ganglion cell death with the loss of visual field sensitivity, those monkeys showing the earliest of field defects had already lost more than 60% of their ganglion cells.[36] Therefore, it is likely that the reductions in COR reported here were due to the loss of afference consequent to the death, rather than the inactivity, of ganglion cells.

The effects of experimental glaucoma reported here are likely to occur clinically, because the characteristics of increasing IOP in the monkey are, in the main, similar to those of clinical glaucoma.[42–44] The main difference is in the time course of the process, which takes only months in monkeys (and with a usually higher elevation of IOP in the monkey) and years in people. Experimentally, these effects on metabolism are much more readily discernable in the monkey model than in human material, because there is always an adjacent target tissue that receives input from a normal companion eye.

Acknowledgments

The authors thank Bryan Ewing and Shilpa Patel for technical and histologic assistance and Alice Chuang for advice on the statistics.

References

1. Krupin T. Trumpeting the perils of glaucoma. In: *13th Biennial Eye Research Seminar.* New York: Research to Prevent Blindness; 1995:62–63.
2. Dreyer EB. Glutamate "excitotoxicity" and glaucoma. In: *13th Biennial Eye Research Seminar.* New York: Research to Prevent Blindness; 1995:63–65.
3. Perkins ES. The Bedford Glaucoma Survey, I: long-term follow-up of borderline cases. *Br J Ophthalmol.* 1975;57:179–185.
4. Kitazawa Y, Horie T, Aoki S, et al. Untreated ocular hypertension. *Arch Ophthalmol.* 1977;95:1180–1184.
5. Armaly MF, Krueger DE, Maunder L, et al. Bio-statistical analysis of the Collaborative Glaucoma Study, I: summary report of the risk factors for glaucomatous visual-field defects. *Arch Ophthalmol.* 1980;98:2163–2171.
6. Quigley HA, Enger C, Katz J, Sommer A, Scott R, Gilbert D. Risk factors for the development of glaucomatous visual field loss in ocular hypertension. *Arch Ophthalmol.* 1994;112:644–649.
7. Levene R. Low tension glaucoma: a critical review and new material. *Surv Ophthalmol.* 1980;24:621–664.
8. Schumer RA, Podos SM. The nerve of glaucoma! *Arch Ophthalmol.* 1994;112:37–44.
9. Gaasterland D, Tanishima T, Kuwabara T. Axoplasmic flow during chronic experimental glaucoma, I, light and electron microscopic studies of the monkey optic nervehead during development of glaucomatous cupping. *Invest Ophthalmol Vis Sci.* 1978;17:838–851.
10. Minckler DS, Spaeth GL. Optic nerve damage in glaucoma. *Surv Ophthalmol.* 1981;26:128–148.
11. Quigley HA, Addicks, EM. Chronic experimental glaucoma in primates, II: effect of extended intraocular pressure elevation on optic nerve head and axonal transport. *Invest Ophthalmol Vis Sci.* 1980;19:137–152.
12. Harwerth RS, Smith EL III, DeSantis L. Visual fields of monkeys with experimental glaucoma. *Invest Ophthalmol Vis Sci.* 1992;33:1162.
13. Quigley HA, Hohman RM. Laser energy levels for trabecular meshwork damage in the primate eye. *Invest Ophthalmol Vis Sci.* 1983;24:1305–1307.
14. Quigley HA., Sanchez, RM, Dunkelberger GR, L'Hernault NL, Baginski TA. Chronic glaucoma selectively damages large optic nerve fibers. *Invest Ophthalmol Vis Sci.* 1987;28:913–920.
15. Glovinsky Y, Quigley HA, Dunkelberger GR. Retinal ganglion cell loss is size dependent in experimental glaucoma. *Invest Ophthalmol Vis Sci.* 1991;32:484–491.
16. Glovinsky Y, Quigley HA, Pease ME. Foveal ganglion cell loss is size dependent in experimental glaucoma. *Invest Ophthalmol Vis Sci.* 1993;34:395–400.
17. Smith EL III, Chino YM, Harwerth RS, Ridder WH III, Crawford MLJ, DeSantis L. Retinal inputs to the monkey's lateral geniculate nucleus in experimental glaucoma. *Clin Vision Sci.* 1993;8:113–139.
18. Vickers JC, Hof PR, Schumer RA, Wang RF, Podos SM, Morrison JH. Magnocellular and parvocellular visual pathways are both affected in a macaque model of glaucoma. *Aust NZ J Ophthalmol.* 1997;25:239–243.
19. Wong-Riley M. Changes in the visual system of monocularly sutured or enucleated cats demonstrable with cytochrome oxidase histochemistry. *Brain Res.* 1979;171:11–28.

20. Wong–Riley M. Cytochrome oxidase: An endogenous metabolic marker for neuronal activity. *Trends Neurosci.* 1989;2:94–101.
21. Wong–Riley M. Primate visual cortex: dynamic metabolic organization and plasticity revealed by cytochrome oxidase. In: Peters A, Rockland KS, eds. *Cerebral Cortex: Primary Visual Cortex in Primates.* Vol. 10. New York: Plenum Press; 1994:141–200.
22. Carrol EW, Wong–Riley M. Quantitative light and electronic microscopic analysis of cytochrome oxidase-rich zones in the striate cortex of the squirrel monkey. *J. Comp Neurol*. 1984;222:18–37.
23. Wong–Riley M, Trusk T, Hoppe D. Localization of cytochrome oxidase in macaque striate cortex during prenatal development. *Soc Neurosci Abstr.* 1988;14:743.
24. Wong–Riley M, Hevner RF, Cutlan R, et al. Cytochrome oxidase in the human visual cortex: distribution in the developing and the adult brain. *Visual Neurosci.* 1993;10:41–58.
25. Wong–Riley M, Carroll EW. The effect of impulse blockage on cytochrome oxidase activity in the monkey visual system. *Nature.* 1984;307:262–264.
26. Wong–Riley MTT, Tripathi SC, Trusk TC, Hoppe DA. Effect of retinal impulse blockage on cytochrome oxidase-rich zones in the macaque striate cortex, I: quantitative EM analysis of neurons. *Visual Neurosci.* 1989;2:483–497.
27. Wong–Riley MTT, Trusk TC, Tripathi SC, Hoppe DA. Effect of retinal impulse blockage on cytochrome oxidase-rich zones in the macaque striate cortex, II: quantitative EM analysis of neuropil. *Visual Neurosci.* 1989;2:499–514.
28. Di Rocco RJ, Kageyama GH, Wong–Riley MTT. The relationship between CNS metabolism and cytoarchitecture: a review of ^{14}C-deoxyglucose studies with correlation to cytochrome oxidase histochemistry. *Comp Med Imaging Graph.* 1989;13:81–92.
29. DeYoe EA, Trusk TC, Wong–Riley MTT. Activity correlates of cytochrome oxidase-defined compartments in granular and supragranular layers of primary visual cortex of the macaque monkey. *Visual Neurosci.* 1995;12:629–639.
30. Hendrickson AE, Tigges M. Enucleation demonstrates ocular dominance columns in Old World macaque but not in New World squirrel monkey visual cortex. *Brain Res.* 1985;333:340–344.
31. Tigges M, Hendrickson AE, Tigges J. Anatomical consequences of long-term monocular eyelid closure on lateral geniculate nucleus and striate cortex in squirrel monkey. *J Comp Neurol*. 1984;227:1–13.
32. Crawford MLJ, Carter–Dawson L, Shen F, Smith EL III, Harwerth RS. Experimental glaucoma in monkeys: effects on magno- and parvo-cellular afferent pathways [ARVO Abstract]. *Invest Ophthalmol Vis Sci.* 1998;39(4):**S**692. Abstract nr 3176.
33. Harwerth RS, Smith EL, DeSantis L. Experimental glaucoma: perimetric field defects and intraocular pressure. *J Glaucoma.* 1997;6:390–401.
34. Kalloniatis M, Harwerth RS, Smith EL, DeSantis L. Colour vision anomalies following experimental glaucoma in monkeys. *Ophthalmic Physiol Opt.* 1993;13:56–67.
35. Malpeli JG, Baker FH. The representation of the visual field in the lateral geniculate nucleus of *Macaca mulatta. J Comp Neurol*. 1975;161:569–594.
36. Harwerth RS, Carter–Dawson L, Shen F, Smith EL, Crawford MLJ. Ganglion cell losses underlying visual field defects from glaucoma. *Invest Ophthalmol Vis Sci.* 1999;40:2242–2250.
37. Crawford MLJ. Column spacing in normal and visually deprived monkeys. *Exp Brain Res.* 1998;123:282–288.
38. Johnson CA. Selective versus nonselective losses in glaucoma. *J Glaucoma*. 1994;3(suppl. 1):S32–S44.
39. Quigley HA, Dunkelberger GR, Green WR. Chronic human glaucoma causing selectively greater loss of large optic nerve fibers. *Ophthalmology.* 1988;95:357–363.
40. Lund JS. Anatomical organization of macaque monkey striate visual cortex. *Annu Rev Neurosci.* 1988;11:253–288.
41. Weber AJ, Kaufman PL, Hubbard WC. Morphology of single ganglion cells in the glaucomatous primate retina. *Invest Ophthalmol Vis Sci.* 1998 39:2304–2320.
42. Pederson JE, Gaasterland DE. Laser-induced primate glaucoma, I: progression of cupping. *Arch Ophthalmol.* 1984;102:1689–1692.
43. Radius RL, Pederson JE. Laser-induced primate glaucoma, II: histopathology. *Arch Ophthalmol*. 1984;102:1693–1698.
44. Koss MC, March WF, Nordquist RE, Gherezhiher T. Acute intraocular pressure elevation produced by argon laser trabeculoplasty in the cynomolgus monkey. *Arch Ophthalmol.* 1984;102:1699–1703.